Scanning Microscopy

Volume 1992
Number 6 *Signal and Image Processing in Microscopy and Microanalysis*

Article 26

1992

The Detection and Quantification of Straight-Lined Irregularities on Surfaces

J. Alan Swift
Unilever Research Port Sunlight Laboratory, England

Scanning Microscopy Supplement 6, 1992 (pages 283-291) 0892-953X/92$5.00+.00
Scanning Microscopy International, Chicago (AMF O'Hare), IL 60666 USA

THE DETECTION AND QUANTIFICATION OF STRAIGHT-LINED IRREGULARITIES ON SURFACES

J.Alan Swift

Unilever Research Port Sunlight Laboratory, Quarry Road East, Bebington, Wirral, L63 3JW, England

Telephone No.: 051 471 3101 Fax No.: 051 471 1800

Abstract

Under the microscope, scratches or abrasions on hard otherwise flat surfaces are usually revealed as straight-lined irregularities. At a more macroscopic level creases in thin sheets such as of paper and textile fabrics are also observed to be straight-lined. A computer-aided image analytical method is described here not only for identifying such features but also for counting them, measuring their lengths and evaluating their contrast. Further measures are derived that are in accord with the qualitative visual impact of each line within the milleau of lines in the original image. The method makes use of a parametric transformation from two orthogonally-illuminated images of the surface using the equation $p=x.\cos(\theta) + y.\sin(\theta)$ where x,y are image coordinates, θ is the angle that a straight line makes with the x-axis and p is the perpendicular distance of that line from the coordinate origin. As distinct from the well-known Hough transform, estimates are made for θ at all points in the initial images that are illuminated at a low angle from two orthogonal directions.

KeyWords: Computer image analysis, scratches, creases, straightlines, Hough parametric transform, fabrics.

Introduction

Under the microscope, scratches and abrasions on otherwise smooth surfaces are usually observed to be straight-lined; as too on a more macroscopic scale are creases in thin materials such as paper or textile fabrics that have been loosely flattened out after folding. In both cases the irregularities often run in different angular orientations across the surface, crossing each other in the process. The former are straight-lined because at the magnification of observation the original process of scratching had involved fast linear abrasive motion with little if any component of angular acceleration, and the latter are straight-lined because of topological constraints of the folding process.

In subjective evaluations of such surfaces, it is customary to use a low angle of illumination to highlight the irregularities and to rotate the plane of the specimen with respect to the illumination. This latter condition is required because linear features parallel to the direction of illumination will exhibit little if any contrast but contrast will be maximal where the illumination falls perpendicularly to the feature. Our subjective assessment in these cases involves the unconscious integration of information from a multitude of images at different orientations.

The use of computer-aided image analysis for the fully-automated evaluation of the above types of roughened surface and for the measurement of the severity of each separate linear irregularity in them, requires much to be taken into account. This is particularly so where one of the aims of the present work was to seek measures that would correlate with subjective evaluations from the same specimens. Cursory examination of images from typical specimens shows that they are complex and unlikely to yield to simple methods of image analysis. There is on the other hand one property of the images that is of value and that is that the features we wish to quantify are straight-lined in character. A suitable image analytical approach would be to specifically seek these lines. The Hough parametric transform (Hough, 1962; Duda and Hart, 1972) and the related Radon transform (Deans, 1981) are well-known techniques for detecting straight lines in images and there are many fine examples in the literature of their application (e.g. Murphy, 1982; Skingley and Rye, 1987). The equipment we had in hand did not readily lend itself to the Hough or Radon methods

and so we have sought and describe here an alternative approach. This bears some resemblance to the Hough method with the exceptions that at an early stage estimates are made of angular orientations by using two orthogonally-illuminated images of the specimen and that much further processing is required beyond the construction of the parametric transform. The full step-by-step details of the method are described below (a summary computational flow chart is shown in figure 1). The methods have been satisfactorily applied to the fully-automated quantitative measurement of creases in textile fabrics; the results for these are presented. The general scheme is likely to be applicable in other situations such as the measurement of abrasions and scratches on surfaces observed under light or scanning electron microscopes.

Equipment And Software

All the image processing operations described in this paper were carried out with the aid of a series 1 IBAS2 image analysis system from Kontron Electronics of Munich. More specifically, the equipment consisted of a Zilog Z80A-based processor (8-bit, CP/M operating system) with many operations effected through a pipelined array processor (10 Mips) and with peripherals that included a real-time (i.e. 25Hz) 16-bit arithmetic image processor, 4 Mbytes of direct-access image memory, and some further intermediate image storage via a 10 Mbyte Bernoulli disk. In all the present work, images of 8 bits depth were acquired via a TV camera (Chalnicon) by averaging 16 frames on the real-time processor. All programmes for the job were written in Fortran making extensive use of manufacturer's software libraries that for many of the high-speed arithmetic operations appropriately load the array processor. Most images used in the work were of square format 512 x 512 picture points by 8 bits depth (i.e. 256 levels of brightness) but for some of the operations intermediate images of up to 32 bits depth were used to preserve accuracy (this was particularly the case for the parametric transform accumulator). A schematic of the set-up under which low-angle illuminated images of the starting fabric pieces were acquired is shown as part of figure 1.

Computational Scheme

Initial estimates of local contrast gradients, G_r and of angular orientations, θ

As mentioned earlier the linearly-disposed irregularities of the specimen are highlighted by their local image contrast where illuminated at a low angle but of a contrast magnitude that varies according to the direction of the illumination. Since our visual evaluation of the magnitude of a given linear feature on the surface is probably attuned to the maximum contrast with the illumination perpendicular to the feature, it seemed to be appropriate initially to make estimates of this maximum contrast for all points in the image field. The most convenient way of doing this was to work with two starting images,

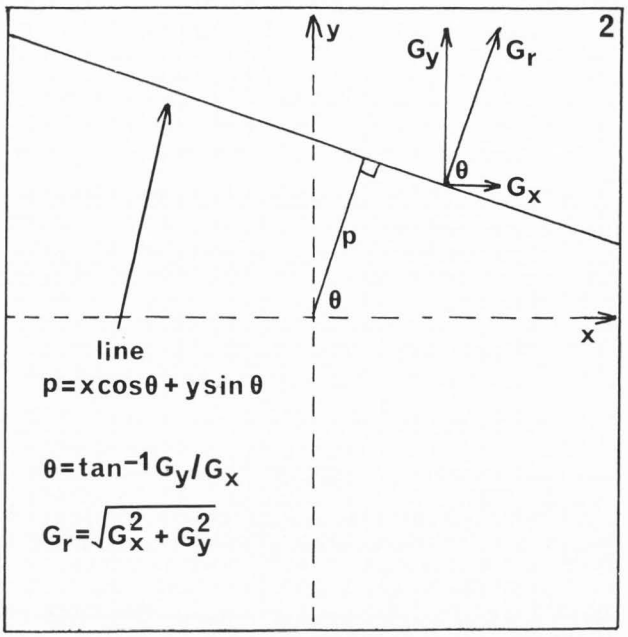

Figure 2: Diagram of an image field in Cartesian (x,y) coordinates with a straight line whose equation is given by $P = x.\cos\theta + y.\sin\theta$ where the parameters P and θ are respectively the perpendicular distance of the line from the origin and the angle that this perpendicular makes with the x-axis. Also illustrated is how angle θ at a point on the line is estimated from a knowledge of the local image intensity gradients in the x- and y-directions, G_x and G_y respectively.

one with the specimen illuminated in the x-direction and the other illuminated in the y-direction. To maintain picture point correspondence between the images the illumination was moved between the capture of the two images whilst a fixed relationship was maintained between the sample and the camera (c.f. figure 1). Proceeding from the first of these images a 'gradient' image G_x was computed that for all its picture points contains the local intensity gradient in the x-direction. A similar 'gradient' image G_y was computed for the corresponding intensity gradients in the y-direction. Using G_x and G_y images a further 'gradient resultant' image G_r was derived (c.f. figure 2) such that picture point for picture point

$$G_r = \sqrt{G_x^2 + G_y^2} \quad \text{---- (1)}$$

Image G_r now contained estimates of the maximum in the local contrast for all angular rotations of the direction of illumination i.e. in a direction roughly perpendicular to each straight-lined irregularity.

For the actual evaluation of G_x and G_y, the following digital convolution filter described by Zuniga and Haralick (1987) was used because of its

Figure 1: Top right is a diagram of the illumination set-up. Starting top left is the computational flow chart leading to the final table of results. N.B. Frames with axes x,y denote 'image' space; those with axes P,θ denote 'transform' space.

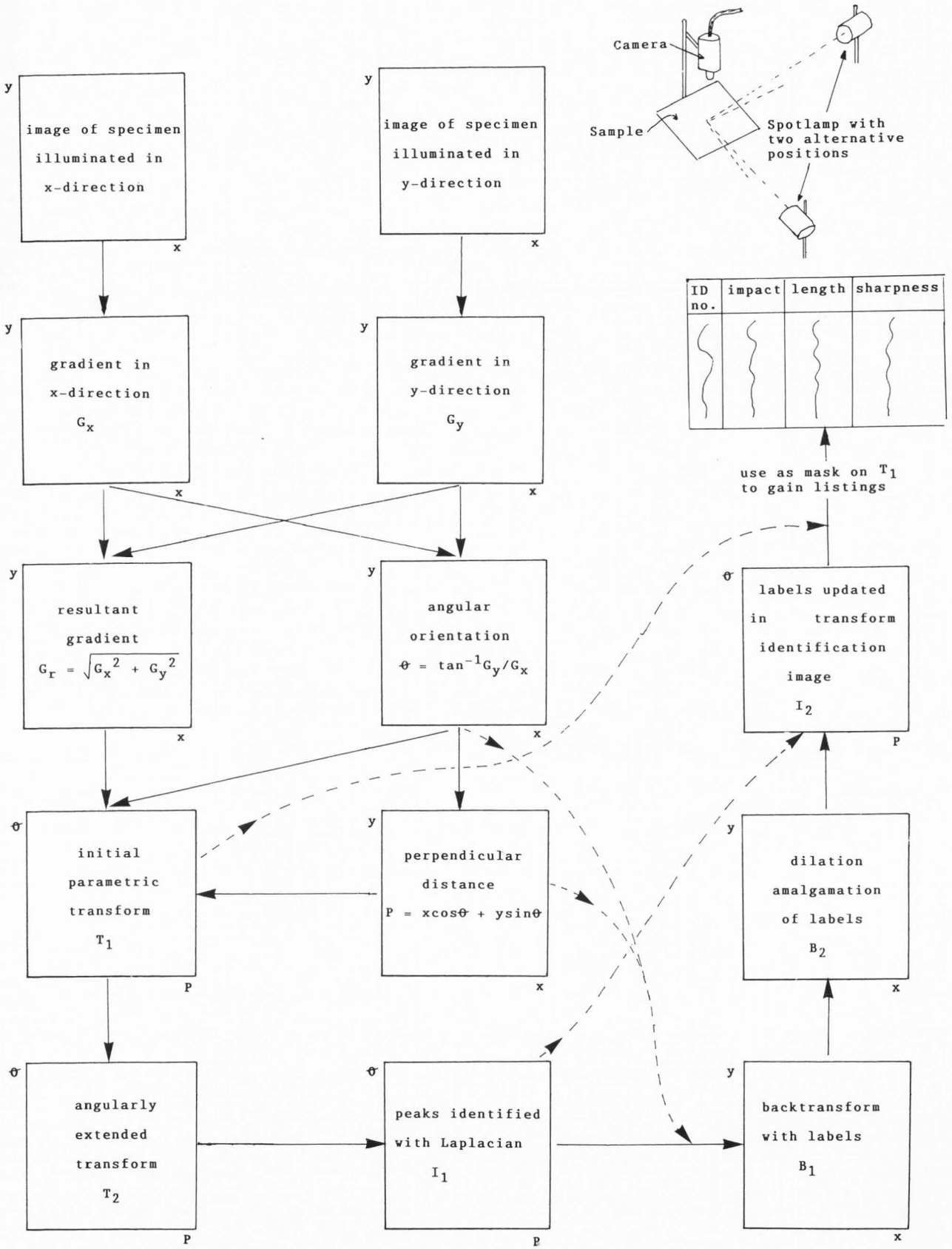
image of specimen illuminated in x-direction
image of specimen illuminated in y-direction
Camera
Sample
Spotlamp with two alternative positions
ID no.
impact
length
sharpness
gradient in x-direction G_x
gradient in y-direction G_y
use as mask on T_1 to gain listings
resultant gradient $G_r = \sqrt{G_x^2 + G_y^2}$
angular orientation $\theta = \tan^{-1} G_y/G_x$
labels updated in transform identification image I_2
initial parametric transform T_1
perpendicular distance $P = x\cos\theta + y\sin\theta$
dilation amalgamation of labels B_2
angularly extended transform T_2
peaks identified with Laplacian I_1
backtransform with labels B_1

claimed high accuracy:

8	-16	0	16	-8
-10	-25	0	25	10
-16	-28	0	28	16
-10	-25	0	25	10
8	-16	0	16	-8

In addition to G_r yet another image was computed picture point for picture point from G_x and G_y namely the angle θ that the resultant vector G_r makes with the x-axis of the image i.e.

$$\theta = \tan^{-1}(G_y/G_x) \text{ ----- (2)}$$

Both G_r and θ are required in the later construction of a parametric transform. In passing it is worth noting some interesting features about θ: a) picture points along each linear feature of the original specimen will tend to have the same value for θ, b) there will be a different value for θ from one line to another (unless they are all parallel!) and c) picture points not on linear surface irregularities will tend to be randomly disposed towards θ.

In our case angles θ were computed to the nearest interval of 0.5^o in the range 0.0 - 179.5^o (noting also that insofar as the angular orientation of the perpendicular to a straight line is concerned 0.0^o is contiguous with 180.0^o).

Estimates of parameter P

The equation for a straight line can be described in terms of parameter θ, the angle that the perpendicular to the line makes with the x-axis and a second parameter P, that is the perpendicular distance in units of interpixel spacing from the line to the origin (0,0) in a system of Cartesian coordinates (x,y) such that

$$P = x.\cos\theta + y.\sin\theta \text{ ------ (3)}$$

A schematic diagram of this relationship is shown in figure 2. If we take as the Cartesian origin the centre of our image field (there are good reasons for choosing this point that will not be elaborated here), then for all picture points in the image field we know the coordinate values (x,y) and the corresponding values for θ (from the θ image computed earlier) and so we can compute using equation 3 yet a further image that contains all the corresponding P data -- we'll call this the P-image.

Construction of the parametric transform T_1

To obtain a parametric transform based upon equation 3 one starts with a two-dimensional accumulator with all possible values for θ (in the present case from 0.0^o to 179.5^o in intervals of 0.5^o) along one axis and all possible values of P (in the present case 512 intervals between $-256\sqrt{2}$ and $+256\sqrt{2}$) along the other axis and all positions within the accumulator initialised to zero. In the simplest process of transformation one sequentially moves through every point within the original images, picks up the corresponding values for θ and P (from the θ- and P-images respectively) and increments the corresponding look-up position in the accumulator array by one. Since picture points along any one linear irregularity within the original image tend to have associated with them the same θ and P values but θ and P off the lines are far more random then this is manifested by a peak in the accumulator at the θ,P position corresponding to the parameters for that particular line. Indeed at the end of the transformation process, a different peak is produced in the accumulator for each and every straight-lined irregularity in the original image.

From such an accumulator (a regular image store was used for the job), the number of peaks in principle identifies the number of straight-lined irregularities in the original sample and the θ,P value at the maximum for each peak tells us, via equation 3, the analytical geometric course of each line across the original image field. More interestingly, the integral under each peak gives an indication of the number of picture points from the original image field that contributed to that peak (i.e. some rough measure of the importance of the corresponding straight feature in that image).

One of the difficulties in using the aforementioned 'pixel count' parametric transform was that it is noisy and, whilst there is no difficulty in deciding which peaks belong to the major linear features on the original specimen, less pronounced linear features are difficult to identify reliably. A modification was made to the parametric transformation that dramatically improved this situation. This was that instead of incrementing the accumulator by unity for each point in the original image field, the corresponding value for G_r (from the G_r image computed earlier) was added. Since G_r is greatest where there are irregularities in the specimen surface but G_r is low on the smoother featureless parts of the specimen, this alternative process served to amplify the peaks whilst distributing the information from the smoother parts of the image more widely and with less intensity about the rest of the transform field i.e. considerable improvement of signal/noise. This alternative transform (referred to as the T_1-image) was more amenable to the quantitative extraction of information about the straight-lined irregularities.

An interesting feature of the alternative transform, that was used to great effect, is that the integral under each peak contains a convolution of the number of picture points belonging to the irregularity in terms of its length and width and the local contrast or sharpness. This has led to the interesting concept of an 'impact measure' i.e. that the integral offers the prospect for a quantitative measure of the irregularity as it might relate to a subjective rating for the importance of the same feature in normal visual scrutiny of the specimen.

Automatic identification of peaks in the transform field

This has proved to be the most difficult part of the overall scheme but, with some ancillary back-transform processing that will be described later, has been satisfactorily resolved.

In the process of identifying peaks in the θ,P parametric transform field of T_1 one needs to take due account of those peaks that straddle the boundary between $\theta = 0.0^o$ and $\theta = 179.5^o$ for these will be split between the two ends of the transform field. To do this it is convenient to artificially extend the transform beyond the normal 179.5^o limit by copying in to it data from the first 20^o from the other end of the transform field (giving a new image T_2). Having identified and numerically labelled the regions bounding each

peak in the extended transform field (see below), it is then neccessary to detect those that specifically straddle the $0.0^{o}/179.5^{o}$ boundary at the point of extension. In the final peak-identification image (I_1), the portions of the 'straddle' peaks extending beyond 179.5^{o} are copied back at the 0^{o}-end of the field and then everything beyond 179.5^{o} is eliminated altogether. This procedure ensures that all relevant peaks are identified and that no peak is counted twice.

The actual method for identifying the areas embracing each peak involved the application of a Laplacian convolution filter to the angularly-extended parametric field (i.e. T_2-image) after it had been linearly compressed to an image of 8 bits depth. The digital convolution filter used was:

0	5	11	14	11	5	0
5	16	19	16	19	16	5
11	19	-23	-62	-23	19	11
14	16	-62	-124	-62	16	14
11	19	-23	-62	-23	19	11
5	16	19	16	19	16	5
0	5	11	14	11	5	0

Where the result was less than or equal to zero, the corresponding pixels in the output image were set to 1's, else zero. In this image, isolated regions contain clusters of 1's with zeros separating the clusters. Each cluster of 1's roughly identifies each individual straight-lined irregularity in the original image. It is a simple matter by conventional image analysis to identify each separated cluster of 1's, to numerically flag each cluster sequentially and in a further image set the picture points associated with each cluster to the flag number, else zero. We'll call this latter the 'I_1-image', noting also that much utility follows from the use of it.

In principle, the I_1-image enables us to count the number of straight-lined irregularities identified in the original image (i.e. the maximum label value present), to determine from the centre of gravity of each labelled region, the corresponding θ,P values for the analytical course of each line in the original image and, by using each of the flag values in turn as a mask to overlay the earlier T_1-image, to gain an integral that is some quantitative impact measure for each line. There were however some further difficulties that needed to be overcome.

Parametric back-transformation

This process, carried out in conjunction with the I_1-image described earlier, provides the means for ascertaining the fidelity of detection of straight lines by the forward parametric transformation. Following an initial forward transformation to the point of obtaining the I_1-image, a second transform was carried out again in much the same way. Instead of incrementing the parametric accumulator for each x,y point in the original image, the identification value at the appropriate θ,P position in the I_1-image was read and copied back to the corresponding x,y position in another new image where all the points in it had been initially set to zero. This new image (referred to as the B_1-image), maps exactly with the original specimen images and contains the numeric labels at its picture points for each and every straight-lined feature identified by the parametric transformation.

Using colour look-up tables, one can examine the correspondence between labelled peaks in the I_1-image and the picture points (of the same colour) that gave rise to them with the B_1-image. Furthermore it is a simple matter to compare each line thus identified in the B_1-image with the information contained within the original images.

In seeking to identify creases in textile fabrics, an immediate problem was discovered; namely that the parametric transform process had been so sensitive that not only were the straight-lined creases identified but also the high frequency linear warp and weft structure of the fabric itself. This problem was immediately remedied by removing the high frequency information from the initial orthogonally-shadowed images by passing a 5 x 5 median convolution filter over each of them at the outset. Having eliminated this problem another one was revealed in the B_1-image; namely that more straight lines were being identified than were visibly present in the original sample. A redeeming feature about this (as considered further in the next section) was that whilst each prominent linear feature tended to be uniquely labelled, the 'extra' lines were manifested as short linear sections closely adjacent to or indeed enmeshed with the major linear features albeit with quite separate identification labels. By scrutinising the B_1 transform field, it was clear that this problem had arisen as a consequence of shortcomings of the Laplacian peak-identification process; i.e. sometimes shoulders to peaks in the transform field were identified and labelled as separate from the main peak.

Final image processing and presentation of results

A suitable strategy was adopted for tidying up the B_1-image that enabled the problem identified in the previous section to be overcome and for a satisfactory conclusion to be reached for the overall image analytical method development.

Each label was considered in turn in the B_1-image according the number of picture points in the image for that label. Starting with the label with the highest number of points, the corresponding picture points were dilated by two steps on an octagonal former. If the dilated regions embraced more than 50% of the picture points for other labels, then those labels were considered to belong to the labels of the dilation set and so the corresponding picture points were reassigned to that for the dilation label. This process was iterated throughout the remaining labels and by way of rigour a second complete pass was made through the labels. This gave rise to a new set of labellings in 'image' space referred to as B_2. The overall result of these manipulations was quite dramatic for now each and every linear discontinuity in the images of the original specimen was uniquely and unambiguously labelled in B_2. In the course of this process, account was kept of the label amalgamations for it was then necessary to carry out the same label amalgamations within image I_1 (the original identification image in transform P,θ space) to derive a new one, I_2.

Proceeding from these latter operations various pieces of quantitative information were derived using B_2 and I_2. These were:

a) a count of the number of linear features i.e. the number of labels contained within the final B_2-image.

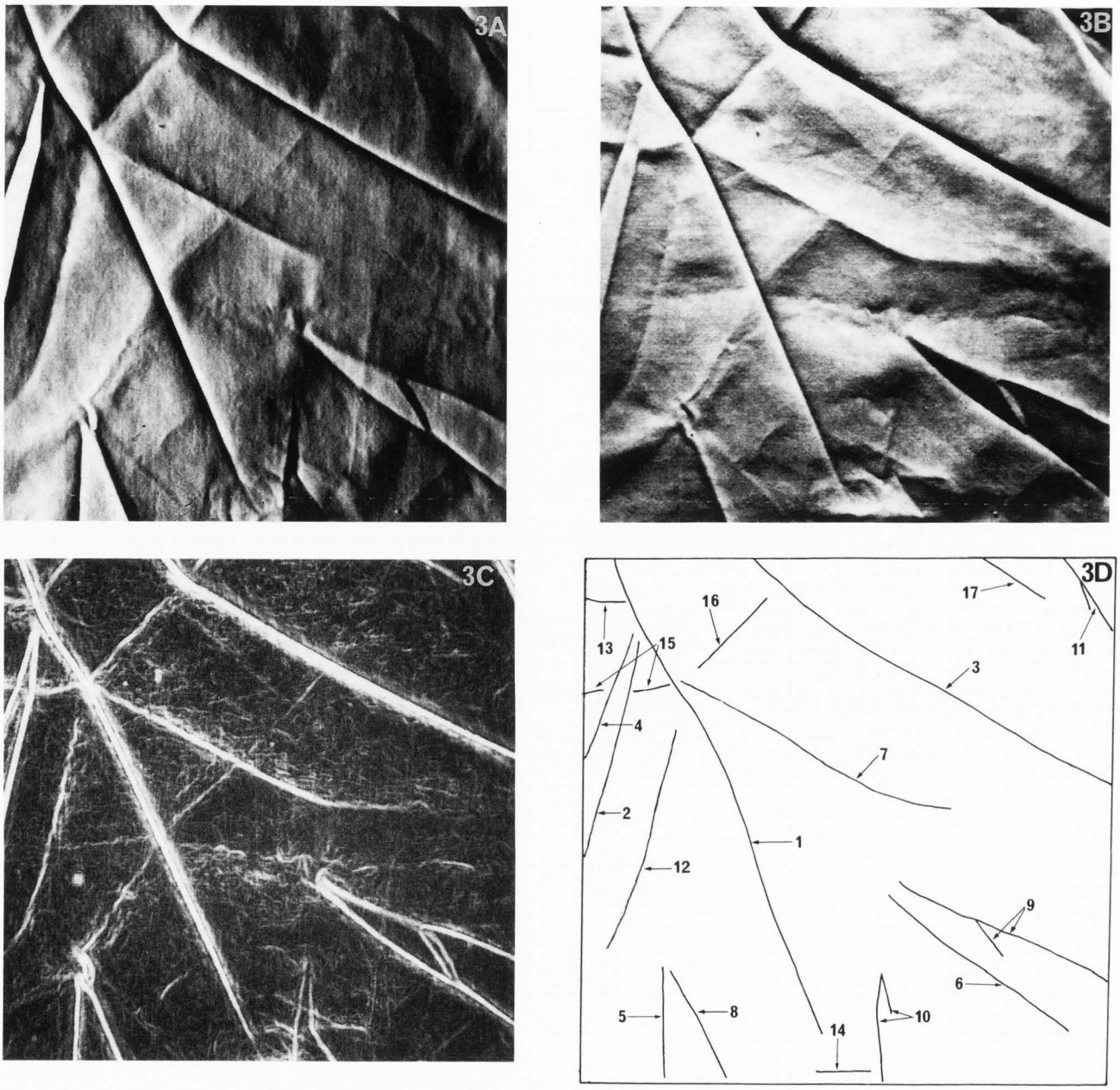

Figure 3: A and B are starting images of a creased fabric piece illuminated in orthogonal directions (x- and y-directions respectively). C is the corresponding 'gradient resultant' image G_r derived by using images A and B. In D the creases and identification numbers for this same specimen are shown as they appeared in the final stage of the image processing operations. The identification numbers relate to results in table 1. Image fields all of side 175 mm.

b) a measure of the 'impact value' for each feature. Taken as the integral under the T_1-image by masking with the amalgamated feature labels in the I_2-image.
c) a simple measure of the length of each feature as the maximum distance between pixels of corresponding label in the B_2-image.
d) a simple measure of feature 'sharpness'. Taken as the estimated impact value for that feature divided by its estimated length.

Computational efficiency

The foregoing methods clearly involve a great deal of computation. In the initial stages of development, a 'blunderbus' approach was taken with little regard for computational efficiency. In consequence, it took 4 hours to obtain the answers for each specimen! Some economies were subsequently effected that gave 35 minutes/sample; sufficient for our initial purposes. These included constraining integer arithmetic throughout and the use of pre-calculated look-up

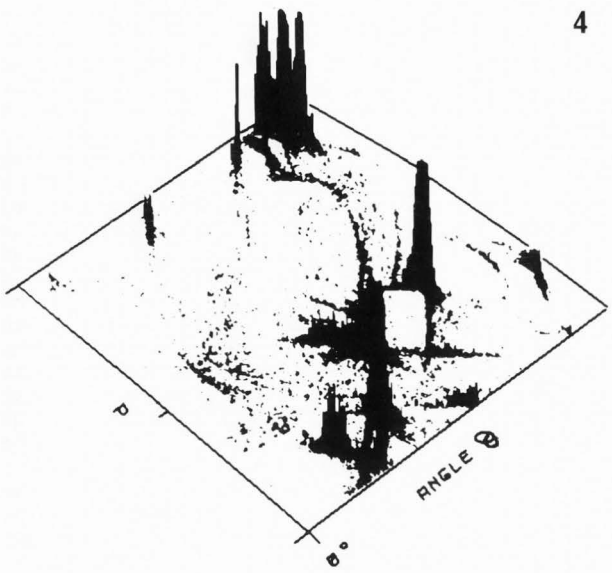

Figure 4: Isometric projection of the P,Θ parametric transform obtained by using the starting images shown in figures 3A and 3B.

tables in the evaluation of equations 1 and 2.

At present major rate-limiting steps occur at four points in the computional scheme; namely in the evaluation of equations 1 and 2 for the whole image and in both the forward- and back-transforms. All these operations involve some kind of look-up operation that at the moment has to be carried out one pixel at a time throughout the whole image field. Thus for example in the evaluation of the G_r-image according to equation 1, pixel by pixel the value for G_x is read from the G_x-image, then the corresponding value for G_y is read from the G_y -image, these are then referred to a pre-calculated 2-D look-up table to read off G_r and then this is written into the corresponding position of the G_r-image. Our newer series 2 IBAS2 equipment from Kontron (MS/DOS, 'C' programming and a compiler for the pipelined-array processor) is basically faster than the series 1 machine (on which the original method development was carried out). We are confident that the rate-limiting steps could be effectively dealt with by undertaking the look-up operations by appropriate programming of the pipelined-array processor. We estimate that these further improvements should permit measurement speeds of the order of 20 seconds/sample; in our experience this is quite adequate for routine evaluation work.

Results

The aforementioned parametric transformation and image processing operations have been used for the fully-automated measurement of creases in textile fabrics. Typical examples of starting images from a creased sample of 50:50 polyester:cotton woven plain-white fabric are shown in figures 3A and 3B (illuminated in the x-direction and y-direction respectively), the corresponding 'gradient resultant' image is shown in figure 3C and the P,Θ parametric transform is shown in isometric projection in figure 4. Figure 3D illustrates the creases automatically identified by the process and Table 1 shows, for the numeric labels of the creases in figure 3D, the corresponding measures for each crease of impact, length and sharpness. The values in this table are in complete accord with one's expectations for the creases in the original specimen.

Table 1: Listing of results for the identification and measurement of creases in the fabric sample whose starting images are shown in figures 3A and 3B and according to the crease identity numbers shown in figure 3D.

Crease ident. no.	Measures* obtained for each crease of:		
	Impact	Length	Sharpness
1	5112	515	9.9
2	3809	281	13.6
3	3385	443	7.6
4	1838	153	13.4
5	1441	100	12.0
6	1219	306	4.0
7	1011	296	3.4
8	834	131	6.4
9	684	312	2.2
10	605	172	3.5
11	526	162	3.2
12	293	218	1.3
13	80	37	2.2
14	71	106	0.7
15	68	37	1.8
16	61	90	0.7
17	41	47	0.9

* - instrumental internal self-consistent units

Discussion

Whilst we have not examined any other types of specimens, it is our belief that the methods described here will be applicable to other types of samples and, in the context of the present conference, probably to the evaluation of straight-lined scratches and abrasions on otherwise smooth surfaces observed under the microscope. Our experience is that the method is sufficiently sensitive to be able to cope with the multiplicity of scratches normally found in such specimens.

The results shown in Table 1, taken in conjunction with figures 3 A-D, are typical of the many fabrics samples we have examined and attest to the power of the present parametric transform method for the automatic evaluation of creases. They provide us for the first time with the ability to relate objective measures of creases to consumer evaluations of the visible state of the same fabric pieces and to elucidate what physical characteristics about the fabrics cause particular subjective judgements to be made about them. Notable amongst the measures is that of 'impact'; this conveniently seems to embrace the same sort of criteria (about crease length, width and sharpness) by which the evaluator visually assesses the relative importance of different kinds of creases in fabrics.

Finally it is worth pointing out that one of the particular merits of the present parametric

method (as is also true for the Hough and Radon methods) is that the straight lines in the starting images need not be continuous to be sensitively detected. Indeed in the present case the fabric creases are discontinuous at a local level not only on account of local variations in fine fabric texture but also because of angular intersections of the creases. By any other conventional method of image analysis (e.g. discrimination according to image intensity or intensity gradient and the need to associate many disconnected segments) the task would have been difficult, if not impossible.

Acknowledgments

Particular thanks are due to my colleagues Drs. Brian Duffin and Steve Joyce. It was Dr. Duffin who initially brought to my attention the need for an instrumental method to be developed for the evaluation of creases in textile fabrics and for the measurement of individual creases in them. It was he who supplied me with suitable samples for measurement. Dr. Joyce was quite invaluable in suggesting, and in some cases providing, solutions to some of the computational difficulties encountered in the course of the present work. Thanks are also due to Dr. R.Davies of Royal Holloway and New Bedford College, Egham, Surrey, England for his suggestion that accuracy of the transform is optimal where the origin of the Cartesian coordinates is taken as the geometric centre of the starting images. It was also his suggestion that better results might be obtained by accumulating image contrast rather than numbers of picture points in the transform process.

References

Deans SR. (1981). Hough transformfrom the Radon transform. Trans.IEEE. PAMI-3, 185-188.

Duda RO, Hart PE. (1972). Use of the Hough transformation to detect lines and curves in pictures. Graphics and Image Process. 15, 11-15.

Hough PVC. (1962). Method and means for recognising complex patterns. US Patent. 3069654.

Murphy LM. (1982). Linear feature detection and enhancement in noisy images via the Radon transform. Patt.Recognit.Lett. 4, 279-284.

Skingley J, Rye AJ. (1987). The Hough transform applied to SAR images for thin line detection. Patt.Recognit.Lett. 6, 61-67.

Zuniga OA, Haralick RM. (1987). Integrated directional derivative operator. Trans.IEEE. SMC-17, 508-517.

Discussion with Reviewers

N.K.Tovey: Adequate contrast in the images is essential otherwise the accuracies to 0.5^{o} cannot be justified using the Zuniga and Haralick filter.
Author: We took great pains to ensure accuracy in the use of the Zuniga and Haralick filter. Indeed we ascertained with the aid of straight lines scored on a flat-surfaced specimen in known orientations that the method we were using (the full details for which were not included in the paper) was capable of better than 0.5^{o} accuracy.

The problem to which Dr. Tovey alludes is that as the gradient in either one of the two orthogonal directions approaches zero, the error of the angle calculated about the particular picture point increases insofar as this is affected by the ratio of the two gradients from which the angle is evaluated via the tangent function. What is pertinent to our solution of this problem of calculating the angles is that it doesn't matter what greater value the two gradients take providing the same underlying operations are carried out in evaluating each of them that preserves the ratio between them. The accuracy of evaluating the angle thereby can be increased. A satisfactory solution was achieved through the use of a series of convolution filters for the Zuniga and Haralick function with different arithmetic divisors. The results for the different divisors were suitably masked in pairs for x-direction and y-direction gradients so that the maximum gradient in either was between the decimal value 128 and 255 in the 8-bit store without actually exceeding 255. Satisfactory precautions were also taken to ensure that the contrast in the initial captured images of the specimen fell within the maximum dynamic range for the system.

It is also worth mentioning in the present context that where, for a given divisor in the gradient convolution filter, both gradients about given picture points are of very low value as compared with the gradients at other picture points, this signifies parts of the specimen that are relatively flat and featureless and of little concern to us. These picture points can sometimes constitute a significant proportion of the image area and so it is worthwhile excluding them from the parametric transform process in the interests of increasing the speed of the whole operation.

N.K.Tovey: Many researchers tackling the problem of directional statistics, and in particular the difficulty when 180^{o} is approached have used the trick first suggested by Curray (1956). In this the directions are artificially transformed by multiplying them by 2 for calculations of resultant vectors etc. At the end, the resultant direction is halved. To avoid the difficulty highlighted by the author which was overcome by the T_2 image, it should be possible to generate an accumulator P,θ where the values of θ have been multipled by 2. This accumulator is then transformed into polar space, and the polar image used directly for the peak search, without the need for two stages of copying. Has the author tried an approach such as this?
Author: Thank you for your suggestion; we will try it.

N.K.Tovey: In figures 3A and 3B there appears to be a diagonal crease running approximately through the centre from bottom left to top right. This does not appear on figure 3D. Is there a reason for this?
Author: There is indeed a simple reason and that is, for expeditiously preparing diagrams and tables that were not too cluttered by detail, a cut-off was applied to omit creases of low impact measures. It happens that the crease in question was one that was identified in our complete work as the next in the sequence of diminishing impact values but has been excluded by the cut-off. It is worth emphasising in the present context that our method is capable of discriminating the finest of real creases and far more in fact than one might be led to believe from figure 3D.

J.D.Fairing: How was figure 3D generated?
Author: This was traced from the image I_2 (of the scheme shown in figure 1) and the lines numbered according to the colour-coded identification numbers displayed in I_2.

S.M.Montgomery: The convolution shown appears to be the one for G_x. Is it readily understood that the filter for G_y would be a rotation of the one shown?
Author: You are correct in thinking that this may not so readily be understood. In point of fact, the convolution filters for the equipment on which we did this work set negative results to zero and so it was necessary to carry out the operation with the basic filter shown with its pixel weightings rotated through each of 90^o and then appropriately meld the angular results into one image store by masking operations.

S.M.Montgomery: I agree that a line may be represented by singular values of θ and P, where P is the perpendicular distance from the line to the origin (0,0). In the paragraph following Equation (3), however, it reads as if, for every (x,y) point on a line, one would use the coordinate values x,y along with θ in Equation (3) to calculate a given value of P. Maybe a differentiation in nomenclature between (x,y), the coordinate values of any point in the image, and (x',y'), the intersection point of the line of interest and a line emanating from the origin at an angle θ, would clarify this. I don't see how you could get a constant P for a line if you used (x,y) values along the line, rather than (x',y').
Author: To answer your question it is perhaps worth clarifying the parametric transformation process used here because no assumptions are made about the pre-existence of lines in the image that would lead us to consider another set of coordinates x'y'. Notably every picture point in the image is treated as if it belonged to a straight line passing through that point according to its (x,y) coordinate in image space and an estimate of the local orientation about it derived by using equation (2). This orientation (θ) is one of our two main parameters for the parametric transform. Equation (3), impresses our considerations of straight lines in the image and gives rise to the second calculated parameter, P, that will be associated with each and every picture point in original image space. The corresponding P and θ values for all the picture points are referred, in the basic transform process, to P,θ in parametric space where the number count is accumulated. Had the starting object been randomly and finely granular without straight-lined detail, the surface of the P,θ accumulator would have been relatively smooth because the values of P and θ are random. On the other hand, as soon as a single straight line is introduced into the starting image(s), this results in a significant greater proportion of the picture points possessing the same (or similar) P and θ values. This in turn causes specific peaking in the P,θ transform accumulator above the otherwise random background. The P,θ position of this peak via equation (3) informs us of the analytical course of the line in the original image. In the case of our fabrics there will be roughly as many peaks in the transform as different straight-lined creases in the original sample.

S.M.Montgomery: I like your use of G_r as a multiplier in the θ,P field to increase signal-to-noise.
Author: Thank you.

S.M.Montgomery: How do you decide if lines 9, 10 and 11 are actually 1, or 2 lines? It appears that the two different sections that make up the line have very different q values.
Author: I didn't decide but rather that was the classification shown as a result of the automated procedure. Your question on the other hand does raise the interesting issue as to whether or not it would have been desirable for the two component parts on each of lines 9, 10 and 11 to have been identified separately. I have no fixed view on this matter except to say the secondary branches in each case are such minor components of the whole image and of 'impact' very much less than for the more major creases, that the error is probably insignificant. This kind of effect has not troubled us in our overall evaluations of creasing in textile fabrics.